JACS
JOURNAL OF THE AMERICAN CHEMICAL SOCIETY
Communication
pubs.acs.org/JACS

Enzyme Architecture: Optimization of Transition State Stabilization from a Cation−Phosphodianion Pair

Archie C. Reyes, Astrid P. Koudelka, Tina L. Amyes, and John P. Richard*

Department of Chemistry, University at Buffalo, SUNY, Buffalo, New York 14260-3000, United States

Supporting Information

ABSTRACT: The side chain cation of R269 lies at the surface of L-glycerol 3-phosphate dehydrogenase (GPDH) and forms an ion pair to the phosphodianion of substrate dihydroxyacetone phosphate (DHAP), which is buried at the nonpolar protein interior. The R269A mutation of GPDH results in a 110-fold increase in K_m (2.8 kcal/mol effect) and a 41 000-fold decrease in k_{cat} (6.3 kcal/mol effect), which corresponds to a 9.1 kcal/mol destabilization of the transition state for GPDH-catalyzed reduction of DHAP by NADH. There is a 6.7 kcal/mol stabilization of the transition state for the R269A mutant GPDH-catalyzed reaction by 1.0 M guanidinium ion, and the transition state for the reaction of the substrate pieces is stabilized by an additional 2.4 kcal/mol by their covalent attachment at wildtype GPDH. These results provide strong support for the proposal that GPDH invests the 11 kcal/mol intrinsic phosphodianion binding energy of DHAP in trapping the substrate at a nonpolar active site, where strong electrostatic interactions are favored, and obtains a 9 kcal/mol return from stabilizing interactions between the side chain cation and transition state trianion. We propose a wide propagation for the catalytic motif examined in this work, which enables strong transition state stabilization from enzyme−phosphodianion pairs.

The large 11−13 kcal/mol binding energy of the phosphodianion group of substrates for triosephosphate isomerase (TIM),[1] orotidine 5′-monophosphate decarboxylase (OMPDC),[2] and L-glycerol 3-phosphate dehydrogenase (GPDH)[3] (Scheme 1) is used to drive an energetically demanding change in structure, which locks their substrates in a protein cage.[4−6] We are interested in understanding the mechanism by which this *investment* in binding energy is *returned* as stabilization of the transition state for these enzymatic reactions.[7−9] Figure 1A shows the surface of yeast OMPDC (*Sc*OMPDC) from an X-ray crystal structure of the complex with the tight-binding inhibitor 6-hydroxyuridine 5′-monophosphate (BMP).[5] The phosphodianion gripper loop (Pro202-Val220) and pyrimidine umbrella (Glu152-Thr165), shaded red, trap BMP in a protein cage, and the guanidinium ion side chain of R235, shaded black, forms an ion pair with the substrate phosphodianion.[5] The R235A mutation at *Sc*OMPDC results in an 1200-fold increase in K_m and a 15-fold decrease in k_{cat} for decarboxylation of OMP, corresponding to a 5.6 kcal/mol destabilization of the transition state.[10] There is strong activation of the R235A mutant enzyme by the added guanidinium cation (Gua^+), and 1 M Gua^+ stabilizes the decarboxylation transition state by 3.0 kcal/mol.[11]

Scheme 1

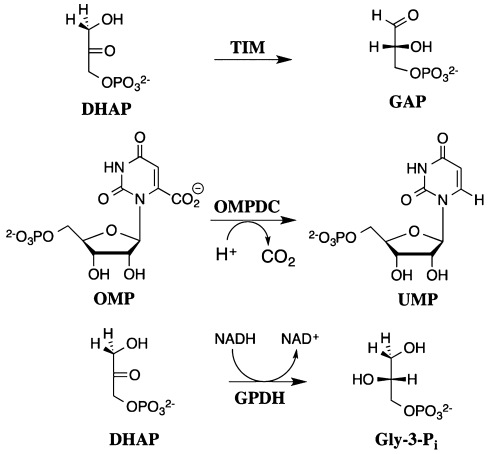

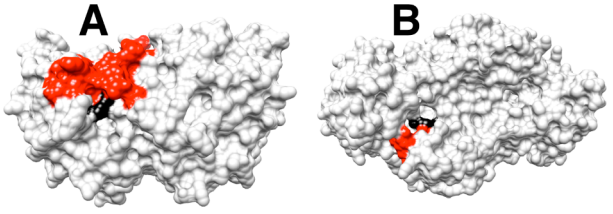

Figure 1. Representations, from X-ray crystal structures, of the surfaces of enzyme-ligand complexes: the loops that trap the ligand in a catalytic cage are shaded red, and the guanidine side chains at the protein surface are shaded black. (A) The complex between ScOMPDC and 6-hydroxyuridine 5′-monophosphate (BMP) (PDB entry 1DQX). (B) The nonproductive ternary complex of dihydroxyacetone phosphate (DHAP) and NAD^+ with *hs*GPDH (PDB entry 1WPQ).

Figure 1B shows the surface of human L-glycerol 3-phosphate dehydrogenase (*hs*GPDH), from an X-ray crystal structure of the nonproductive ternary complex with substrate dihydroxyacetone phosphate (DHAP) and the oxidized nicotinamide cofactor NAD^+.[6] The loop (Leu292-Leu297, shaded red) locks the ligand in a protein cage, while the guanidinium ion side chain of R269 (shaded black) forms an ion pair with the substrate phosphodianion. There are no direct interactions between the phosphodianion and "capping" loop of GPDH.

Received: March 1, 2015
Published: April 17, 2015

DOI: 10.1021/jacs.5b02202
J. Am. Chem. Soc. 2015, 137, 5312−5315

Table 1. Effect of the R269A Mutation on the Kinetic Parameters and Activation Barriers for Reactions Catalyzed by Wildtype *hs*GPDH at pH 7.5 (triethanolamine buffer), 25 °C, and I = 0.12 (NaCl)

	Kinetic Parameters and the Effect of Gua^+ on the Activation Barriers[a]								
GPDH	k_{cat} (s^{-1})[b]	$\Delta\Delta G^{\ddagger}$ (kcal/mol)[c]	K_m (M)[b]	$\Delta\Delta G^{\circ}$ (kcal/mol)[c]	k_{cat}/K_m (M^{-1} s^{-1})[b]	$\Delta\Delta G^{\ddagger}$ (kcal/mol)[c]	$(k_{cat}/K_m)_{Gua}/K_d$ (M^{-2} s^{-1})[d]	$\Delta G^{\ddagger}_{Gua}$ (kcal/mol)[e]	$\Delta G^{\ddagger}_{S}$ (kcal/mol)[f]
WT[g]	240		5.2×10^{-5}		4.6×10^{6}				
R269A	$(5.9 \pm 0.4) \times 10^{-3}$	6.3	$(5.7 \pm 0.5) \times 10^{-3}$	2.8	1.0 ± 0.15	9.1	$(8.0 \pm 0.5) \times 10^{4}$	−6.7	2.4

[a]The uncertainty in the kinetic parameters is the standard error from least-squares fits of the kinetic data. [b]Kinetic parameter for *hs*GPDH-catalyzed reactions at a saturating concentration of NADH. [c]Effect of the mutation on ΔG for the reaction in the previous column. [d]Third-order rate constant for activation of *hs*GPDH by Gua^+. [e]Equation 2. [f]Equation 4. [g]Data from ref 12.

This suggests that the loop functions to sequester DHAP from solvent at the relatively nonpolar active site cage.[7] The similarity between the positioning of capping loops relative to the side chain cation for OMPDC and GPDH prompted the prediction of a similar role for these side chain cations in catalysis.[12] We report results, which confirm this prediction, and a discussion of the origin of catalytic power of the motif shown in Figure 1.

Wildtype GPDH from human liver (*hs*GPDH) was cloned and overexpressed.[12] The enzyme was assayed at pH 7.5 (100 mM triethanolamine buffer) and I = 0.12 (NaCl) by monitoring the oxidation of NADH by DHAP.[3] Standard protocols were followed (Supporting Information) in constructing, expressing, and purifying the R269A mutant of *hs*GPDH from *Escherichia coli* that also contained host *ec*GPDH. The crude protein mixture obtained from an ammonium sulfate fractionation was twice purified over a Q-sepharose ion-exchange column. The host *ec*GPDH apparently eluted first, and the mutant *hs*GPDH eluted from the second Q-sepharose column with a constant *apparent* specific activity of 0.001 units/mg.

GPDH-catalyzed reduction of DHAP follows an ordered kinetic mechanism, with the NADH cofactor binding first to the enzyme.[13] The Michaelis–Menten plot of initial velocity data (v/[E] against [DHAP]) for R269A mutant *hs*GPDH-catalyzed reduction of DHAP carried out using either 0.10 or 0.20 mM NADH (Figure S2) shows an excellent fit to the single set of kinetic parameters k_{cat} and K_m reported in Table 1: this is consistent with $K_m \ll 0.10$ mM for NADH. A comparison of the kinetic parameters for wildtype and R269A mutant *hs*GPDH (Table 1) shows that the mutation results in a 4.6×10^6-fold decrease in k_{cat}/K_m, which is divided between 110-fold and 40 000-fold, respectively, changes in K_m and k_{cat}.

There is no detectable activation of wildtype GPDH by the guanidinium ion (Gua^+), but the activity lost upon the R269A substitution is rescued, with unusual efficiency, by binding of Gua^+ from solution (Supporting Information).[14,15] Figure 2 shows the effect of increasing [Gua^+] on the second-order rate constant $(k_{cat}/K_m)_{obs}$ for *hs*GPDH-catalyzed reduction of DHAP. The values of $(k_{cat}/K_m)_{obs}$ for reactions in the presence of different fixed [Gua^+] were determined as the slopes of the linear correlations from Figure 2A. Figure 2B shows the effect of increasing [Gua^+] on $(k_{cat}/K_m)_{obs}$. The slope of the linear correlation at [Gua^+] < 0.05 M is equal to the third-order rate constant $(k_{cat}/K_m)_{Gua}/K_d = 8.0 \times 10^4$ M^{-2} s^{-1} for activation (Scheme 2). The slight downward curvature for reactions in the presence of high [Gua^+] (dashed line, Figure 2B) is due to either weak saturation of *hs*GPDH by Gua^+ or the specific salt effect of replacing NaCl by $Gua^+ \cdot Cl^-$.

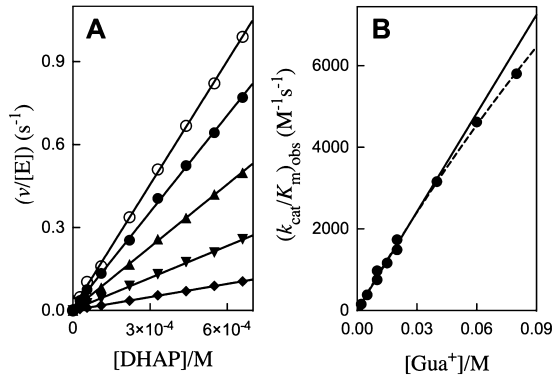

Figure 2. Effect of Gua^+ on R269A mutant *hs*GPDH-catalyzed reduction of DHAP by NADH for reactions at pH 7.5 (20 mM triethanolamine buffer), 25 °C, saturating [NADH] = 0.2 mM, and I = 0.12 (NaCl). (A) The increase in v/[E] (s^{-1}), with increasing [DHAP], for reactions at different fixed [Gua^+]: (◆) 2 mM Gua^+; (▼) 5 mM Gua^+; (▲) 10 mM Gua^+; (●) 15 mM Gua^+; (○) 20 mM Gua^+. (B) The effect of increasing [Gua^+] on the values of $(k_{cat}/K_m)_{obs}$ from Figure 2A.

Scheme 2

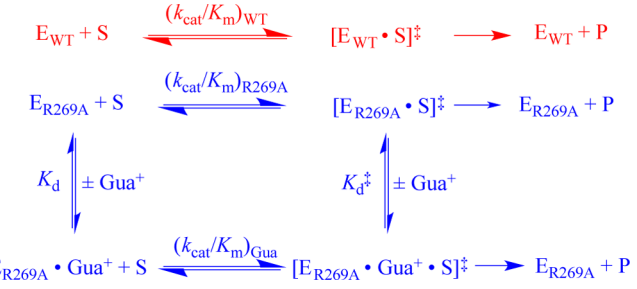

The efficacy of activation of R269A mutant *hs*GPDH by Gua^+ and the advantage from covalent attachment of the activator to the enzyme are quantified, respectively, by two parameters, $\Delta G^{\ddagger}_{Gua}$ and $\Delta G^{\ddagger}_{S}$ (eqs 1–4, derived for Scheme 2).[16,17] The first parameter, $\Delta G^{\ddagger}_{Gua}$ = −6.7 kcal/mol (Table 1), is determined from the ratio of the third-order rate constant $(k_{cat}/K_m)_{Gua}/K_d$ for rescue of R269A mutant *hs*GPDH by Gua^+ and the second-order rate constant $(k_{cat}/K_m)_{R269A}$ for the *unactivated* mutant enzyme-catalyzed reaction (eqs 1 and 2). This ratio is equal to $1/K_d^{\ddagger}$ for *release* of Gua^+ from the transition state for the mutant enzyme-catalyzed reaction (Scheme 2) and, therefore, defines the *stabilization* of the transition state by interaction with 1.0 M Gua^+ (Table 1).

The second parameter, $\Delta G^{\ddagger}_{S}$, is determined from the ratio of the second-order rate constant $(k_{cat}/K_m)_{WT}$ and the third-order rate constant $(k_{cat}/K_m)_{Gua}/K_d$ for rescue of R269A mutant

DOI: 10.1021/jacs.5b02202
J. Am. Chem. Soc. 2015, 137, 5312–5315

*hs*GPDH by Gua^+ (eqs 3 and 4). This rate constant ratio is equal to the "effective molarity" (EM, eq 3) of the Gua^+ side chain of Arg269 at wildtype *hs*GPDH.[18] Equation 4 shows the relationship between the EM and $\Delta G^{\ddagger}_{S}$, where the latter is the apparent transition state stabilization provided by a covalent connection between Gua^+ and the R269A mutant *hs*GPDH.[19] This connection, in effect, converts the mutant pieces to the whole wildtype *hs*GPDH. Equation 5 partitions the 9.1 kcal/mol overall effect of the mutation on the activation barrier for *hs*GPDH-catalyzed reduction of DHAP into the portion *rescued* by 1 M activator ($-\Delta G^{\ddagger}_{Gua}$ = 6.7 kcal/mol) and the advantage to the intramolecular reaction ($\Delta G^{\ddagger}_{S}$ = 2.4 kcal/mol).

$$\frac{(k_{cat}/K_m)_{Gua}/K_d}{(k_{cat}/K_m)_{R269A}} = \frac{1}{K_d^{\ddagger}} \quad (1)$$

$$\Delta G^{\ddagger}_{Gua} = -RT\ln(1/K_d^{\ddagger}) \quad (2)$$

$$EM = \frac{(k_{cat}/K_m)_{WT}K_d}{(k_{cat}/K_m)_{Gua}} = \frac{(k_{cat}/K_m)_{WT}K_d^{\ddagger}}{(k_{cat}/K_m)_{R269A}} \quad (3)$$

$$RT\ln(EM) = \Delta G^{\ddagger}_{S} = (\Delta G^{\ddagger}_{R269A} + \Delta G^{\ddagger}_{Gua}) - \Delta G^{\ddagger}_{WT} \quad (4)$$

$$\Delta G^{\ddagger}_{R269A} - \Delta G^{\ddagger}_{WT} = \Delta G^{\ddagger}_{S} - \Delta G^{\ddagger}_{Gua} = 9.1 \text{ kcal/mol} \quad (5)$$

Scheme 3 shows the effects of R235A[11] and R269A mutations on catalysis by OMPDC and *hs*GPDH, respectively.

Scheme 3

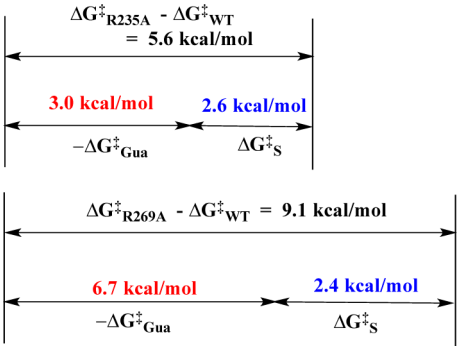

The ion pair between the phosphodianion and the side chain cation of R235 provides a 5.6 kcal/mol stabilization of the transition state for OMPDC decarboxylation, for a case where the side chain interacts essentially exclusively with the phosphodianion at the transition state (Figure 3A).[10,20] There is a larger 9.1 kcal/mol stabilizing interaction between the side chain cation of R269 and the transition state for *hs*GPDH-catalyzed reduction of DHAP, perhaps because the side chain is sufficiently close (5.7 Å from the carbonyl oxygen of DHAP at the nonproductive complex shown in Figure 3B),[6] to interact with both the phosphodianion and the C-2 oxygen, which is partly negatively charged at the transition state for hydride transfer from NADH to the carbonyl oxygen.

We propose that the catalytic motif from Figure 1 has been widely propagated. Triosephosphate isomerase (TIM) is strongly activated for catalysis by a phosphite dianion.[21,22] TIM uses the *surface* cationic side chain of Lys12, which lies adjacent to a dianion gripper loop, to stabilize the transition state for isomerization of DHAP.[23] The K12G mutation results in an 8 kcal/mol destabilization of the enediolate trianion-like

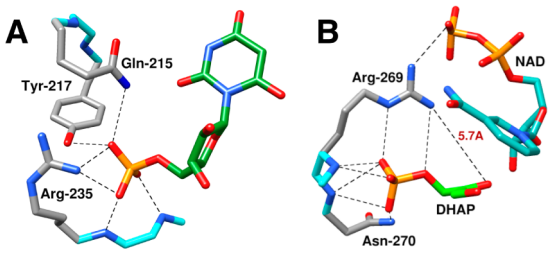

Figure 3. Representations of X-ray crystal structures of *Sc*OMPDC and *hs*GPDH. (A) *Sc*OMPDC in a complex with 6-hydroxyuridine 5′-monophosphate (PDB entry 1DQX). (B) The nonproductive ternary complex of human liver *hs*GPDH with DHAP and NAD^+ (PDB entry 1WPQ).

transition state,[24] from loss of interactions with the side chain cation, and the lost activity is efficiently rescued by alkyl ammonium ions.[16] The complex between a substrate analog and a $(MgF_3)^-$ mimic of phosphorylated β-phosphoglucomutase shows a positioning of the capping loop and the surface side chain of Arg49, which is strikingly similar to that for OMPDC and GPDH (Figure S3).[25] The related enzyme α-phosphoglucomutase has been shown to use phosphodianion binding energy in activation for catalysis.[26]

The results of recent studies on the mechanism of action of ketosteroid isomerase emphasize the dominant role of electrostatic interactions in stabilization of the transition state for enzyme-catalyzed proton transfer.[27,28] Our results emphasize the important role of electrostatic interactions in stabilization of the transition state for an enzyme-catalyzed hydride transfer reaction, while illustrating the power of enzymes to achieve a large rate enhancement from a *single* focused interaction. They provide a textbook example of a catalytic motif, which strongly enhances electrostatic interactions at nonpolar enzyme active sites compared to the polar solvent water.[7,29,30] The weak aqueous interaction between Gua^+ and HPO_4^{2-} (0.6 kcal/mol),[31] or between Gua^+ and an OMP trianion (1.0 kcal/mol),[11] is enhanced dramatically for the interacting surface side chains of R235 and R269 and the buried transition states for the OMPDC- and GPDH-catalyzed reactions.

Our results emphasize the *return* to OMPDC and GPDH from *investment* of the intrinsic dianion binding energy to construct nonpolar caged complexes (Figure 1). This provides these enzymes the benefit of 5.6 and 9.1 kcal/mol stabilization of the respective transition states by strong ion pairing interactions (Scheme 3) between a surface side chain cation and transition state trapped at the protein interior, where the ion pair is strengthened by reduction of the medium dielectric constant compared to water.[7,32] Cage formation activates TIM through an enhancement in the basicity of the carboxylate side chain of E167, which abstracts a proton from enzyme-bound substrate.[33] We note the possibility of a similar return from utilization of *any* set of enzyme−substrate binding interactions to drive the formation of an active caged Michaelis complex, and suggest that this return might be obtained by protein engineers interested in the *de novo* design of proteins with enzyme-like activity.[34]

■ ASSOCIATED CONTENT

Supporting Information

Materials and experimental procedures for the cloning, overexpression, and purification of R269A mutant *hs*GPDH;

DOI: 10.1021/jacs.5b02202
J. Am. Chem. Soc. 2015, 137, 5312−5315

the assay for R269A mutant *hs*GPDH in the presence and absence of $Gua^+ \cdot Cl^-$; Figure S1, elution profiles for purification of R269A mutant *hs*GPDH; Figure S2, Michaelis−Menten plot of $v/[E]$ against [DHAP] for R269A *hs*GPDH; Figure S3, representation of surface of β-phosphoglucomutase. This material is available free of charge via the Internet at http://pubs.acs.org.

AUTHOR INFORMATION

Corresponding Author

*jrichard@buffalo.edu

Notes

The authors declare no competing financial interest.

ACKNOWLEDGMENTS

This work was supported by Grant GM39754 from the National Institutes of Health.

REFERENCES

(1) Amyes, T. L.; O'Donoghue, A. C.; Richard, J. P. *J. Am. Chem. Soc.* **2001**, *123*, 11325−11326.
(2) Amyes, T. L.; Richard, J. P.; Tait, J. J. *J. Am. Chem. Soc.* **2005**, *127*, 15708−15709.
(3) Tsang, W.-Y.; Amyes, T. L.; Richard, J. P. *Biochemistry* **2008**, *47*, 4575−4582.
(4) Joseph, D.; Petsko, G.; Karplus, M. *Science* **1990**, *249*, 1425−1428.
(5) Miller, B. G.; Hassell, A. M.; Wolfenden, R.; Milburn, M. V.; Short, S. A. *Proc. Natl. Acad. Sci. U.S.A.* **2000**, *97*, 2011−2016.
(6) Ou, X.; Ji, C.; Han, X.; Zhao, X.; Li, X.; Mao, Y.; Wong, L.-L.; Bartlam, M.; Rao, Z. *J. Mol. Biol.* **2006**, *357*, 858−869.
(7) Richard, J. P.; Amyes, T. L.; Goryanova, B.; Zhai, X. *Curr. Opin. Chem. Biol.* **2014**, *21*, 1−10.
(8) Amyes, T. L.; Richard, J. P. *Biochemistry* **2013**, *52*, 2021−2035.
(9) Richard, J. P. *Biochemistry* **2012**, *51*, 2652−2661.
(10) Goldman, L. M.; Amyes, T. L.; Goryanova, B.; Gerlt, J. A.; Richard, J. P. *J. Am. Chem. Soc.* **2014**, *136*, 10156−10165.
(11) Barnett, S. A.; Amyes, T. L.; McKay Wood, B.; Gerlt, J. A.; Richard, J. P. *Biochemistry* **2010**, *49*, 824−826.
(12) Reyes, A. C.; Zhai, X.; Morgan, K. T.; Reinhardt, C. J.; Amyes, T. L.; Richard, J. P. *J. Am. Chem. Soc.* **2015**, *137*, 1372−1382.
(13) Bentley, P.; Dickinson, F. M. *Biochem. J.* **1974**, *143*, 19−27.
(14) Toney, M. D.; Kirsch, J. F. *Protein Sci.* **1992**, *1*, 107−119.
(15) Toney, M. D.; Kirsch, J. F. *Science* **1989**, *243*, 1485−1488.
(16) Go, M. K.; Amyes, T. L.; Richard, J. P. *J. Am. Chem. Soc.* **2010**, *132*, 13525−13532.
(17) Olucha, J.; Meneely, K. M.; Lamb, A. L. *Biochemistry* **2012**, *51*, 7525−7532.
(18) Kirby, A. J. *Adv. Phys. Org. Chem.* **1980**, *17*, 183−278.
(19) Jencks, W. P. *Proc. Natl. Acad. Sci. U.S.A.* **1981**, *78*, 4046−4050.
(20) Amyes, T. L.; Ming, S. A.; Goldman, L. M.; Wood, B. M.; Desai, B. J.; Gerlt, J. A.; Richard, J. P. *Biochemistry* **2012**, *51*, 4630−4632.
(21) Go, M. K.; Amyes, T. L.; Richard, J. P. *Biochemistry* **2009**, *48*, 5769−5778.
(22) Amyes, T. L.; Richard, J. P. *Biochemistry* **2007**, *46*, 5841−5854.
(23) Lodi, P. J.; Chang, L. C.; Knowles, J. R.; Komives, E. A. *Biochemistry* **1994**, *33*, 2809−2814.
(24) Go, M. K.; Koudelka, A.; Amyes, T. L.; Richard, J. P. *Biochemistry* **2010**, *49*, 5377−5389.
(25) Jin, Y.; Bhattasali, D.; Pellegrini, E.; Forget, S. M.; Baxter, N. J.; Cliff, M. J.; Bowler, M. W.; Jakeman, D. L.; Blackburn, G. M.; Waltho, J. P. *Proc. Natl. Acad. Sci. U.S.A.* **2014**, *111*, 12384−12389.
(26) Ray, W. J., Jr.; Long, J. W. *Biochemistry* **1976**, *15*, 3993−4006.
(27) Schwans, J. P.; Sunden, F.; Gonzalez, A.; Tsai, Y.; Herschlag, D. *Biochemistry* **2013**, *52*, 7840−7855.
(28) Fried, S. D.; Bagchi, S.; Boxer, S. G. *Science* **2014**, *346*, 1510−1514.
(29) Richard, J. P.; Amyes, T. L. *Bioorg. Chem.* **2004**, *32*, 354−366.
(30) Richard, J. P. *Biochemistry* **1998**, *37*, 4305−4309.
(31) Springs, B.; Haake, P. *Bioorg. Chem.* **1977**, *6*, 181−190.
(32) Malabanan, M. M.; Amyes, T. L.; Richard, J. P. *Curr. Opin. Struct. Biol.* **2010**, *20*, 702−710.
(33) Malabanan, M. M.; Nitsch-Velasquez, L.; Amyes, T. L.; Richard, J. P. *J. Am. Chem. Soc.* **2013**, *135*, 5978−5981.
(34) Zanghellini, A. *Curr. Opin. Biotechnol.* **2014**, *29*, 132−138.

DOI: 10.1021/jacs.5b02202
J. Am. Chem. Soc. 2015, 137, 5312−5315